Self-Organization of Four Symmetric Tri-phenyl-benzene Derivatives

Vassiliki Vergadou,[†] George Pistolis,*[,‡] Adonis Michaelides,[†] George Varvounis,[†] Michael Siskos,[†] Nikos Boukos,[‡] and Stavroula Skoulika*[,†]

Department of Chemistry, University of Ioannina, 45110 Ioannina, Greece, and NRCSR "Demokritos", 15310 Athens, Greece

ABSTRACT: The self-assembly of four symmetrically substituted tri-aryl-benzene derivatives of formula $C_{24}H_{15}X_3$, where X = H (**1**), Cl (**2**), COOMe (**3**), and COOH (**4**), was studied as a function of the substituent X. Crystal packing analysis of compounds **1**−**3** showed that in **1**, there are no strong face-to-face stacking interactions, whereas in both compounds **2** and **3**, molecular columns were formed, held by numerous "lateral" C−H···Cl and C−H···O hydrogen bonds, respectively. However, strong intermolecular face-to-face aromatic interactions, appropriate for excimer formation, were observed only in **3**, in line with results obtained by fluorescence spectroscopy. The π−π aromatic interactions are significantly stronger in the case of the triacid **4**, but a lack of adequate single crystals of this compound prevented any detailed study for correlating crystal architecture with fluorescence emission observed. However, FT-IR and TEM experiments showed the existence of dimeric H-bonds and short (0.35 nm) distances between the phenyl rings.

Introduction

The spontaneous self-assembly of organic molecules into well-defined architectures (in the solid state or in solution) is a topic of intense current research.[1] Molecular organization is achieved through mutual recognition between molecules on the basis of weak intermolecular noncovalent interactions. The manipulation of these interactions in order to direct the assembly process with precision is generally a difficult task. For example, it is not yet possible to routinely predict crystal packing from the knowledge of molecular structure only.[2] These issues are not important only from a fundamental point of view but also for their potential applications, including preparation of new materials for nonlinear optics,[3] nanotubes,[4] molecular zeolites,[5] sensors,[6] etc.

When one type of intermolecular interactions is dominant, it is possible to rationalize or even predict the supramolecular organization. Thus, the so-called chromonic liquid crystal phases are always formed by face-to-face interacting rigid molecules containing several aromatic rings.[7] Strong or conventional O−H···O and N−H···O hydrogen bonds have also been used for the design of organic solids with some predetermined characteristics.[8] However, in the general case, the assembly of organic molecules arises from the interplay of several interactions,[9] and the outcome results from a subtle balance between them. The existence of several polymorphs or pseudopolymorphs for a given compound is probably the most convincing example in these issues.[10]

In the case of conformationally flexible molecules, the conformation itself will also depend on the supramolecular structure and will influence the physical properties of the crystal or aggregate accordingly. In extreme cases, it was observed that a dense hydrogen-bond network can promote the formation of a high-energy coordination sphere in a molecular complex.[11]

In this work, we present a systematic study of the self-assembly of four symmetrically substituted tri-aryl-benzenes
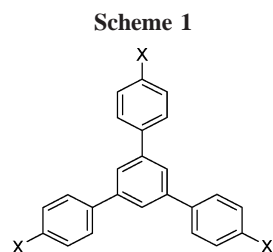
Scheme 1

X=H (**1**), Cl (**2**), COOCH₃ (**3**), COOH (**4**)

(Scheme 1) as a function of the chemical substituent X. We anticipated that the great number of aromatic rings could favor the formation of molecular columns via face-to-face or herringbone interactions, stabilized by "lateral" interactions through weak C−H···halogen, C−H···π, C−H···O, or strong O−H···O hydrogen bonds.[12] The crystal structure of compound **1** has been determined previously.[13] The solid-state structure of compounds **2** and **3** was determined by X-ray crystallography. A crystal structure of the triacid (**4**) as crystallized from DMF was determined some years ago by Weber et al.[14] In this structure, the COOH groups formed strong H-bonds with DMF, which is a hydrogen bond acceptor, and as a result, no polymeric structure through H-bonding between the acid groups was formed. Moreover, no columnar organization was observed. The molecules are nonplanar (the dihedral angle between the central ring and the peripheral ones is 31.8 °), and only one type of stacking interaction was observed between parallel central benzene rings (interplanar distance 3.66 Å) in pairs of molecules. We thus reasoned that if compound **4** was crystallized from water (or alcohol), then a polymeric structure could be formed via ring-type H-bonds, such as those encountered in the crystal structure of trimesic acid.[15] In this case, we expected that, by synergy, the molecules would adopt a quasi-planar conformation and would organize into columns through extensive aromatic interactions. Unfortunately, despite many efforts, no crystals suitable for X-ray analysis have been obtained so far for compound **4**. However, fluorescence spectroscopy experiments carried out on solid samples of compounds **1**−**4** revealed excimer formation only in compounds **3** and **4**, implying

* Corresponding authors. E-mail: vskoul@cc.uoi.gr (S.S.); pistolis@chem.demokritos.gr (G.P.).
† University of Ioannina.
‡ NRCSR "Demokritos".

Table 1.   Crystal and Structure Refinement Data for Compounds 2 and 3

	2	3
empirical formula	$C_{24}H_{15}Cl_3$	$C_{30}H_{24}O_6$
fw	409.71	480.49
cryst syst	orthorhombic	monoclinic
space group	$P2_12_12_1$	$P2/c$
λ (Å)	1.54178	0.71073
a (Å)	14.447(1)	24.488(4)
b (Å)	18.806(1)	4.749(1)
c (Å)	21.515(1)	22.065(3)
β (deg)	90	110.87(1)
V (Å^3)	5845.4(6)	2397.7(7)
Z	12	4
ρ_{calcd} (g cm^{-3})	1.539	1.331
μ (mm^{-1})	2.442	0.093
T (K)	293	293
no. of reflns collected/unique	4691/4651 (Rint=0.0570)	5437/4216 (Rint=0.0384)
refinement	F^2	F^2
final R ind ($I > 2\sigma(I)$)	R1 = 0.0771, wR2 = 0.2009	R1 = 0.0629, wR2 = 0.1791
R (all data)	R1 = 0.1098, wR2 = 0.2521	R1 = 0.1055, wR2 = 0.2244
res. electron density (e Å^{-3})	0.258/−0.307	0.318/−0.201
GOF	1.114	0.927

interplanar distances between parallel aromatic rings not exceeding 3.5 Å.[16] These results are in line with those found by X-ray structural analysis of compounds **1**−**3**. Detailed fluorescence spectroscopy studies carried out on aqueous solutions of **4** at different pH values, along with TEM experiments, revealed, in the case of acidic solutions, extended $\pi-\pi$ stacking and a high degree of aggregate organization.

Experimental Section

Preparations: **[(C₆H₃)(C₆H₅)₃], (1).** It was purchased from Aldrich and further purified by recrystallization from THF.

[(C₆H₃)(C₆H₄Cl)₃], (2). It was synthesized from the reaction of 4-chloroacetophenone with CF₃SO₃H as described in the literature.[17] Recrystallization from toluene gave crystals suitable for X-ray diffraction experiments.

[(C₆H₃)(C₆H₄COOCH₃)₃], (3). It was prepared by esterification of the triacid (**4**). Recrystallization from dioxane gave good crystals suitable for X-ray crystallography.

[(C₆H₃)(C₆H₄COOH)₃·2H₂O], (4). The triacid was prepared as described in the literature.[14] The product was purified by recrystallization from acetic acid. Slow evaporation of an ethanolic solution of the triacid gave very small, well-formed crystals. Their small size prevented us from studying them by X-ray crystallography. Elemental anal. Calcd for **3**·2H₂O: C, 68.49; H, 4.81. Found: C, 68.66; H, 4.44.

Single-Crystal Structure Analysis. Data were collected at room temperature using a Bruker P4 diffractometer with monochromatic CuKα radiation for **2** and MoKα radiation for **3**. The data were corrected for Lorentz and polarization effects. The structures were solved by direct methods using SHELXS-86 as implemented in SHELXL-97 software and refined on F^2 by a full-matrix least-squares method. All non-hydrogen atoms were refined anisotropically. In compound **2**, hydrogen atoms were located on calculated positions and refined isotropically using a riding model. In compound **3**, one phenyl ring and one ester group were located, by difference Fourier maps, on two distinct positions with an occupational factor of 0.5. Because of steric repulsions, the two groups cannot independently occupy both possible positions, i.e., if the phenyl group occupies one position, its neighboring ester group can be found in only one of the two possible positions. Moreover, the two oxygens and the methyl carbon of the ester group bound to the above-mentioned phenyl acquired somewhat large thermal displacement parameters, so we preferred to refine them over two equivalent positions. The hypothesis that the structure should be better refined in a bigger cell has been ruled out after careful examination of the experimental data. Phenyl hydrogen atoms together with those of the nondisordered ester group were located by difference Fourier maps and refined isotropically. Crystallographic data for compounds **2** and **3** are given in Table 1.

Physical Measurements: Combined TG/DTA analysis was performed on a Schimadzu 60 apparatus under an air stream (5 mL/min). FT-IR spectra were recorded on a Perkin-Elmer Spectrum GX FT-IR
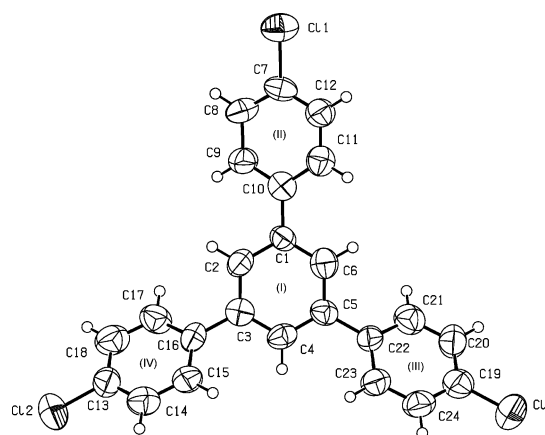

Figure 1. ORTEP plot of one molecule of the asymmetric unit of compound **2**, with the atom numbering scheme and the ring notation.

Table 2.   Interplanar Angles (deg) between the Central Phenyl Ring and the Terminal Ones for Compounds 2 and 3

| | compound 2 | | | |
	molecule A	molecule B	molecule C	compound 3
I−II	24.1(5)	19.2(6)	6.9(7)	9.8(2)
I−III	39.5(5)	44.3(5)	35.9(5)	23.7(3)/30.3(2)
I−IV	33.6(5)	35.7(5)	48.5(4)	36.2(1)

spectrophotometer, using the KBr technique. For absorption spectra, we used the Perkin-Elmer Lambda-16 spectrophotometer. Fluorescence and excitation spectra were recorded on a Perkin-Elmer LS-50B fluorometer. Fluorescence lifetimes were determined using the time-correlated single-photon counter FL900 of Edinburg Instruments. The electron microscopy study was accomplished using a Philips CM20 transmission electron microscope operating at an acceleration voltage of 200 kV.

Results and Discussion

Compound **2** is isostructural to the corresponding bromo compound, obtained by a different synthetic route, whose structure has been published recently.[18] The asymmetric unit is composed of three molecules labeled A, B, and C. The atom-numbering scheme and the ring notation of one of them is presented in Figure 1. The molecules are nonplanar. The interplanar angles between the central aromatic ring and the outer ones for each molecule are given in Table 2. The molecules are arranged, through π-stacking and herringbone
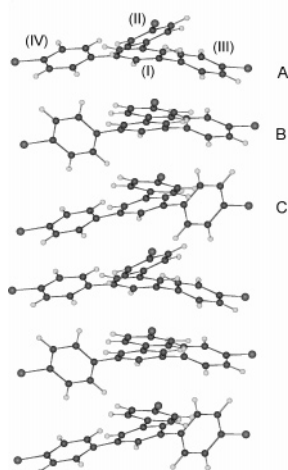
Figure 2. Structure of a molecular column of compound **2**, parallel to the *a* axis. The three molecules A, B, and C of the asymmetric unit are indicated. Selected geometrical parameters between aromatic rings with interplanar distance and angle less than 4 Å and 10°, respectively. (a) Interplanar angles (deg): $I_A–I_C = 5.4$, $IIB–II_C = 2.2$, $III_A–III_B = 6.7$, $IV_A–IV_C = 6.5$, $I_A–II_C = 4.0$, $I_C–II_B = 8.8$, $I_B–II_A = 9.9$. (b) Interplanar distances (Å): $I_A–I_C = 3.5$, $II_B–II_C = 3.5$, $III_A–III_B = 3.9$, $IV_A–IV_C = 3.8$, $I_A–II_C = 3.6$, $I_C–II_B = 3.6$, $I_B–II_A = 3.6$. (c) Slipping distances (Å): $I_A–I_C = 3.1$, $II_B–II_C = 3.4$, $III_A–III_B = 1.6$, $IV_A–IV_C = 1.8$, $I_A–II_C = 3.6$, $I_C–II_B = 1.3$, $I_B–II_A = 1.5$.
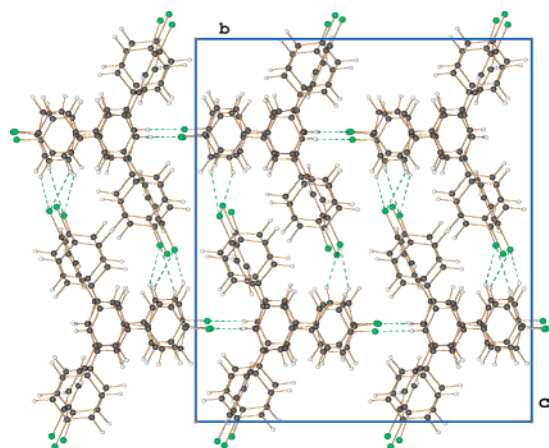

Figure 3. Projection of the structure of compound **2**, along the direction of the columns. The dashed lines represent the C−H···Cl interactions between the columns. Only H···Cl contacts up to 3 Å were considered.

interactions, in columns parallel to the *a* axis (Figure 2). Neighboring chlorine atoms are located at mutual distances of about 4 Å, in line with the so-called chloro-rule.[19] The structure is stabilized by numerous C−H···Cl interactions between neighboring columns (Figure 3).

The asymmetric unit of compound **3** contains one molecule of the triester (Figure 4). The molecule is nonplanar, and the interplanar angles between the central phenyl ring and the outer ones are presented in Table 2. The crystal structure is characterized by the formation of columns parallel to the *b* axis, through essentially face-to-face (I−I and II−II) or nearly face-to-face (I−II) interactions between translationally equivalent molecules (Figure 5). Each molecule is linked to its neighboring ones, belonging to adjacent columns, by numerous C−H···O bonds formed between the ketonic oxygens and phenyl hydrogens (Figure 6). Only two of the three ester groups are involved in H-bonding. The phenyl ring and the ester group presenting disorder do not participate in any appreciable interaction, either aromatic or by H-bonding.
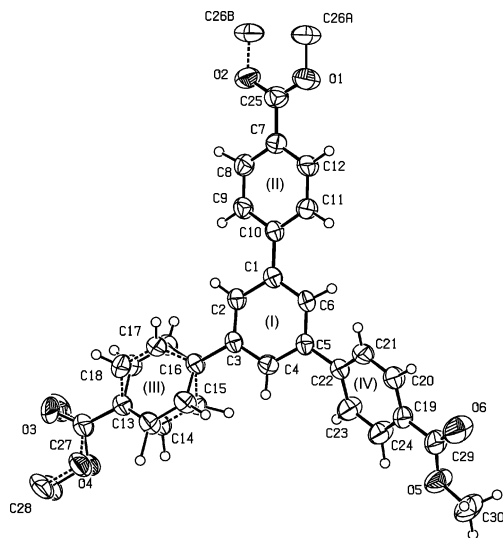

Figure 4. ORTEP plot of the molecular structure of compound **3**, with the atom numbering scheme. The dashed lines represent the second position of the two disordered groups of the molecule.
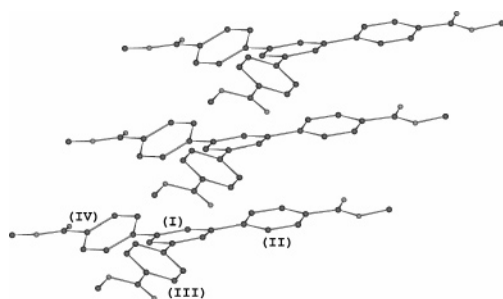

Figure 5. Structure of a molecular column of the triester (**3**), formed parallel to the *b* axis. Selected geometrical parameters between aromatic rings with interplanar distance and angle less than 4 Å and 10°, respectively. (a) Interplanar angles (deg) $I–I' = 0$, $II–II' = 0$, $I–II' = 9.7$. (b) Interplanar distances (Å): $I–I' = 3.5$, $II–II' = 3.5$, $I–II' = 3.4$. (c) Slipping distances (Å): $I–I' = 3.2$, $II–II' = 3.2$, $I–II' = 1.6$.
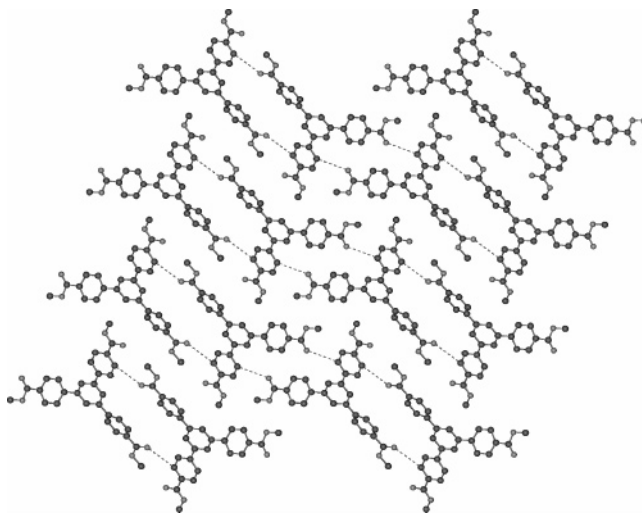

Figure 6. Projection of the structure of compound **3**, along the direction of the columns. Dashed lines represent the C−H···O bonds. Only H···O contacts up to 2.8 Å were considered.

In compound **1**, the molecules are arranged in closely packed layers parallel to the *bc* plane.[13] Successive layers are laterally slipped and, consequently, no characteristic column structure is obtained. The molecules interact by aromatic interactions.
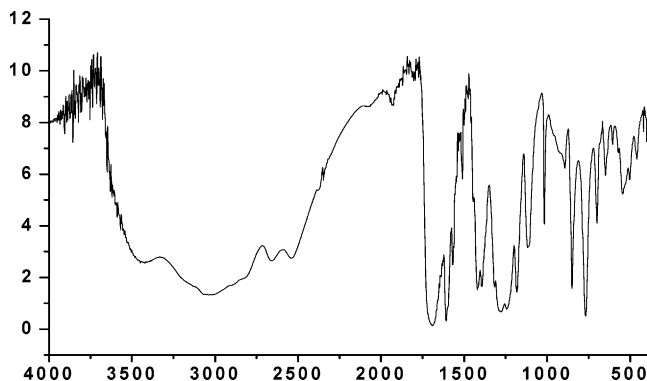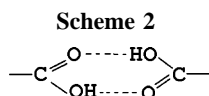
Figure 7. FT-IR spectrum of compound **4**.

Scheme 2

The smaller interplanar angles between phenyl rings are 10.83° (the approximate interplanar distance is 3.73 Å, the lateral offset 3.22 Å) and 11.06° (the approximate interplanar distance is 3.66 Å, the lateral offset 2.39 Å). All other interactions are of the herringbone type[19] (interplanar angle greater than 30°). A first conclusion drawn from the above-described crystal structures is that short interplanar distances (up to 3.5 Å) between strictly parallel aromatic rings belonging to neighboring molecules are present only in compound **3** (triester). These partially overlapped molecular pairs account for the emission properties of this compound in the crystal (vide infra).

As we already mentioned, no crystals of compound **4** suitable for X-ray analysis have been obtained so far. The FT-IR solid state spectra of the acid unambiguously show the presence of hydrogen bonding (Figure 7). The absence of any band above 3500 cm^{-1} shows that there are no "free" OH groups, thereby indicating that all carboxylic groups are hydrogen bonded. The broad peak centered at 3036 cm^{-1}, accompanied by several submaxima up to 2537 cm^{-1}, is characteristic of the well-known R$_2^2$(8) carboxylic acid dimer motif[20] (Scheme 2), with the weaker C$-$H stretching bands probably superimposed upon the broad O$-$H band.[21] This is also supported by the presence of a strong carbonyl ($\nu_{C=O}$) band at 1691 cm^{-1} and of a relatively broad band in the range 905$-$980 cm^{-1} due to the out-of-plane (∂_{OH}) deformation.[21] The ν_{OH} stretching vibration at 3434 cm^{-1} (shoulder) is also indicative of hydrogen bonding but it was not possible to ascribe it with certainty to any well-known interacting pattern (the ν_{OH} due to the so-called catemar motif occurs around 3200 cm^{-1}).[20]

To further investigate the structure of the triacid, **4**, in various environments and conditions, we performed detailed fluorescence studies both in solution and solid state. First, we explored the aggregational behavior of triacid (**4**) in aqueous solution by measuring its fluorescence from an 80/20 water/methanol solution at various pH values (Figure 8). As can be seen, by increasing the pH of the solution (highly basic), the long tail of the red edge of the fluorescence spectrum at pH 7 (solid line) totally disappears and the resulting emission and absorption spectra coincide with those observed for the locally excited state, i.e., monomeric triacid in THF (see also Table 3). On the other hand, at low pH (highly acidic), when all carboxylic groups are nonionized, there is a significant red-shift and broadening of triacid absorption spectrum; its maximum is shifted from 273 to 287 nm, whereas its fwhm increases by 2257 cm^{-1} as compared to those obtained at pH 12. The fluorescence quantum
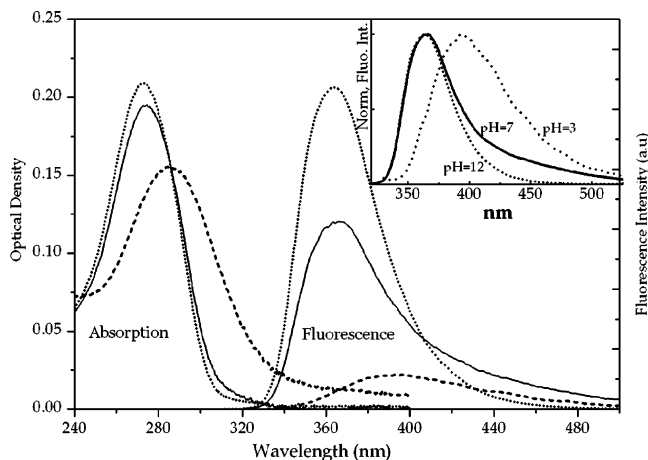

Figure 8. Absorption (left) and fluorescence (right) spectra of 3.3 × 10^{-6} M triacid **4** in an aqueous solution of 80/20 water/MeOH: solid line, pH 7; dotted line, pH 12; and dashed line, pH 3. Inset: Normalized fluorescence spectra as above (excitation at 290 nm).

yield at low pH, on the other hand, drops noticeably (∼75%) and the emission spectrum shows an interesting, new, broad, red-shifted excimer-like emission band centered at ∼396 nm (see inset).

One would argue that this new structureless band at low pH is probably due to extended hydrogen bonding between non-ionized carboxyl groups of triacid **4** and the water/methanol solvents causing perturbations to the spectra. Such a possibility, however, must be excluded, because as shown in Table 3, the presence of ethanol—a solvent with strong hydrogen bonding ability—does not perturb the spectroscopic parameters of triacid, **4**, to an appreciable extent relative to THF. Furthermore, the triacid, **4**, and its methylated derivative, **3**, which has quite different hydrogen bonding properties, show almost identical spectroscopic behavior in both solvents.

To further investigate and clarify the behavior of **4** in the 80/20 water/methanol medium, we performed time-resolved fluorescence studies at different pH levels. The fluorescence decay of triacid, **4**, at pH ∼12 is strictly a single exponential over the whole spectral region studied (τ_f = 23.1 ns, excited at 290 nm). This means that at high pH, when the majority of the carboxylic groups of the triacid are ionized, molecules of **4** repel each other and, consequently, do not form aggregates; instead, they exist in the solution as isolated monomers (see also TEM results). However, at pH ∼7, the decay monitored at 410 nm is analyzed as double-exponential decay consisting of a major component (τ_f = 22.8 ns, 86%) and a minor one (τ_f = 6.0 ns, 14%) whose contribution increases toward the longer wavelengths (see the inset of Figure 8). Finally, at pH ∼3 the "normal" fluorescence decay component ($\tau_f \approx$ 23 ns) totally disappears and the whole spectral region is governed by two decaying components, the aforementioned $\tau_f \approx$ 6.0 ns (∼20%) and an additional slower component $\tau_f \approx$ 12 ns (∼80%).

The dramatic drop in fluorescence quantum yield, the observed red-shift and broadening of the absorption and emission spectra of triacid **4** in aqueous solution at low pH as well as the progressive changes in the time-resolved fluorescence experiments strongly support the formation of interacting couples of triacid molecules in the ground state. In contrast to the highly basic solution, at low pH when all carboxylic groups are in nonionized form and therefore the molecular approach is not hindered by electrostatic repulsion, the fluorescence can be ascribed to some kind of stacking of the molecules. In these stacks, presumably, molecules are arranged in suitable geom-

Table 3. Spectroscopic Parameters of Compounds 1−4 in Different Solvents: Wavelengths (nm) at the Absorption (λ_{abs}) and Emission (λ_{fl}) Maxima (Φ and τ stand for quantum yields and lifetimes (ns) in aerated solvents)

	hexane					THF					ethanol				
sample	λ_{abs}	ϵ_{max}	λ_{fl}	Φ	τ	λ_{abs}	ϵ_{max}	λ_{fl}	Φ	τ	λ_{abs}	ϵ_{max}	λ_{fl}	Φ	τ
1	251	50924	353	0.05	9.4	254	58290	354	0.12	26.2	252	59146	354	0.08	16.1
2	258	70400	359	0.04	5.8	261	73800	360	0.05	8.0	260	75874	360	0.05	7.7
3	273	51700	360	0.11	13.2	278	51400	364	0.19	17.2	276	51100	364	0.15	16.6
4	*a*	*a*	*a*	*a*	*a*	277	50100	363	0.17	17.5	273	64523	368	0.11	11.4

a Not detected because triacid (**4**) is totally insoluble in hexane.
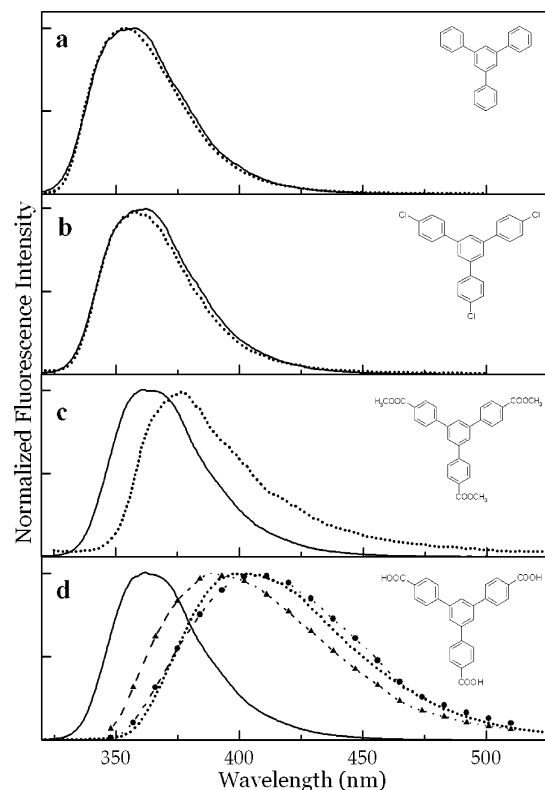
Figure 9. Normalized fluorescence spectra of (a) **1**, (b) **2**, (c) **3**, and (d) **4**, in dilute (3.4×10^{-6} M) THF solutions (solid lines) and in the solid state (dotted lines). Triangles and circles represent normalized time-resolved emission spectra (TRES) constructed from a 3D family of decay curves. The delay times (Δt) and gate widths (δt), respectively, were (s) 3.0 and 1.0 ns and (h) 18.0 and 8 ns.

Table 4. Recovered Decay Times τ (ns) and Percentages (%τ) of the Emitting Species in a Crystalline Film of Triacid (4) and Triester (3) at Various Wavelengths (nm) at an excitation of 300 nm

	τ_1	τ_2	%τ_1	%τ_2	x_v^2
		Compound 4			
375	3.9 ± 0.3	12.3 ± 0.6	34	66	1.03
400	4.2 ± 0.4	13.1 ± 0.6	20	80	1.02
435	4.4 ± 0.4	12.9 ± 0.6	10	90	1.03
480	4.3 ± 0.4	13.3 ± 0.7	6	94	1.07
		Compound 3			
360	3.2 ± 0.3	10.2 ± 0.5	31	69	1.00
380	3.4 ± 0.3	9.6 ± 0.6	38	62	0.97
410	3.7 ± 0.4	9.4 ± 0.6	46	54	1.06
440	4.3 ± 0.4	10.6 ± 0.7	62	38	1.01

(triester), its fluorescence spectrum is noticeably red-shifted by ca. 1025 cm^{-1} relative to the corresponding monomeric spectrum obtained from a dilute solution, although their overlapping remains significant (Figure 9c). However, for compound **4**, viz. triacid, the difference between solution and crystal state spectra is spectacularly increased, reaching a value of ca. 2675 cm^{-1}, resulting in discrete spectral areas (Figure 9d).

The decay curves monitored at various emission wavelengths (see Table 4) are analyzed as double-exponential decays for both compounds. For triester (**3**), the high-energy part of the fluorescence spectrum is governed by a decaying component of ~10 ns, similar to that observed for the locally excited state (monomer fluorescence) in dilute solution (Table 3), i.e., hexane (~13 ns). Consequently, this component is attributed to monomeric fluorescence emitted by molecules not trapped in excimeric states. The second component (~4 ns) becomes predominant toward the red edge of the emission spectrum (low-energy component). Interestingly, for compound **4** (triacid) no monomeric fluorescence can be detected in the crystal state. Instead, its emission shows pure excimeric fluorescence characteristics and consists of a short- and a long-living component of ~4 and ~13 ns, respectively, the latter being predominant as wavelength increases. It is worth noting that the short-living excimeric component (~4 ns) is common in the crystal state of both compounds, namely, triester **3** and triacid **4**, and appears in the spectral region that is determined from the boundaries of the triester's red- and triacid's blue-edge emission spectrum (see panels c and d of Figure 9). In accordance with fluorescence decay analysis, the gated time-resolved fluorescence spectra confirm the existence of two emitting populations in the crystalline state for compound **4**. The early-gated spectrum, which corresponds to fluorescence emitted during the first 1.5−3.1 ns (Figure 9d, ▲), consists principally of the short-living emission state (4 ns). As time elapses, the above emitting species almost disappears and the late-gated spectrum ($\Delta t > 18$ ns, Figure 9d, ●) is composed exclusively from the long-living emitting component (~13 ns). Although crystal data for compound **4** are not available, the almost perfectly alike spectroscopic behavior of the crystals with that of an aqueous solution at pH 3 strongly supports the excimer-like stabilization of the emitting state(s). From our time-resolved experiments,
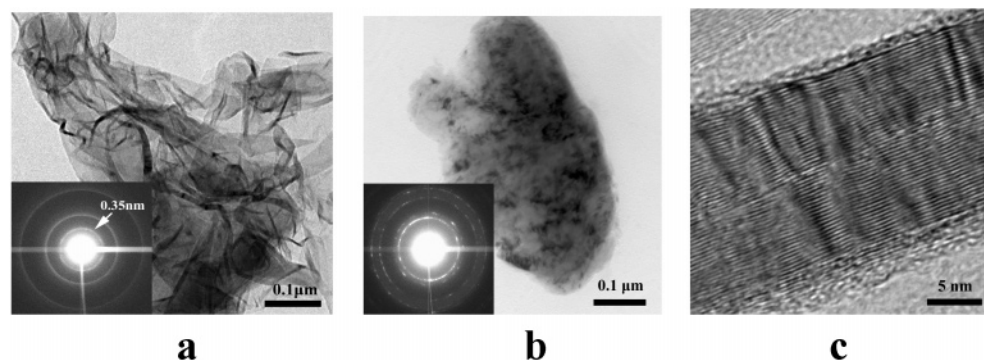
etries for "excimer-like" emission through face-to-face aromatic interactions. It should be noticed that a similar behavior of the absorption and/or fluorescence spectra of various chromophoric systems, which form self-assemblies in appropriate media, is reported in the literature.[16,22]

To further investigate and gain insight into a systematic correlation between crystal structure and emission spectra, we obtained detailed solid-state fluorescence spectra analysis along with the corresponding spectra of **1**−**4** from dilute solutions of 3.4×10^{-6} M in THF (Figure 9). It is clearly seen that the crystal emission of **1** and **2** (panels a and b of Figure 9) is identical with that of the dilute solutions, in which these compounds are dissolved as monomers. Analysis of fluorescence decay traces also confirms the absence of appreciable intermolecular interactions in crystals; in fact, when crystalline films of compounds **1** and **2** are excited at 300 nm and the decay traces are analyzed at various emission wavelengths (335, 355, 375, and 400 nm), a single state of 15 and 3.9 ns for compounds **1** and **2**, respectively, was always detected. On the contrary, the triacid, **4**, and the triester, **3**, show very different spectroscopic behavior in the crystalline state. For compound **3**

Figure 10. Bright field TEM of the triacid (**4**) from a 80/20 water/methanol solution. (a) pH 3, (b) pH 12, and (c) pH 3.

the formation of two types of excimeric sites is demonstrated for triacid, **4**, both in aqueous solution at pH 3 and in the solid state.

The dual excimer emission of various chromophores has been frequently observed not only in organized media in dilute solutions[23] but also in the crystalline state.[24] The simplest form of the excimer state occurs between two nearest neighbor aromatic molecules when the geometrical criterion for sufficient overlapping of π-electron clouds, i.e., interplanar angle near 0° and interplanar distance less than or equal to 3.5 Å,[16] is satisfied. In the so-called sandwich-type arrangement of aromatic moieties, observed in particular in disklike aromatic molecules, i.e., pyrene, perylene, etc., the "perfect" parallel face-to-face arrangement of molecular pairs observed permits a full overlap of aromatic rings, resulting in a discrete low-energy and long-living emission.[23a] On the other hand, it is generally accepted and has spectroscopically been suggested that even a partial overlap, resulting from a slipping of one aromatic moiety relative to the other, of the nearest parallel molecular pairs can lead to the formation of a second excimer. The emission of the latter is quite different from both the monomeric fluorescence and the sandwichlike excimeric one; it appears at higher energy and decays faster than the aforementioned most stable low-energy excimer.[23,24] For example, it has been reported that in some vinyl polymers with pendant carbazoxyl groups, the appearance of the second high-energy excimer may result from the overlap of only one benzene ring in the neighboring chromophores.[23f] It is interesting, therefore, to examine this issue and collect unique information in light of the emissive properties of crystals, at least for compounds **1**–**3**, for which we have solved the crystal structure. In compound **1**, the molecules are arranged in closely packed layers parallel to the bc plane.[13] The smaller interplanar angle between phenyl rings is 10.83° (approximate interplanar distance of 3.73 Å). Therefore, the geometrical criterion for obtaining sufficient overlapping of π-electron clouds is not satisfied for this compound. Furthermore, in compound **2** (Figure 2), the most favorable interplanar arrangement is characterized by an interplanar angle of 2.2°, an interplanar distance of 3.5 Å, and a slipping distance of 3.4 Å. This arrangement is a limiting case; however, fluorescence spectroscopy does not show any excimer formation, and consequently, it is concluded that there is no sufficient π-electron overlapping between adjacent molecules. As previously mentioned, both compounds **1** and **2** emit monomeric fluorescence from their locally excited state, similar to that observed when the molecules exist in a solution as isolated monomers. The most interesting and revealing case is that of the triester crystal structure. As shown in Figure 5, two of the rings (I and II) show a more favorable interplanar arrangement (interplanar angle of 0°, interplanar distance of 3.5 Å, and slipping distance of 3.2 Å)

than in **2**. This partial ring overlap should be responsible for the formation of the aforementioned short-living (4 ns) excimer state, observed in both the steady-state and time-resolved experiments, confirming the nature of this short-living excimer as proposed in earlier studies.[23,24]

In the case of the triacid, **4**, although crystal data are not available, the very large red shift, by more than 2600 cm^{-1} of the solid-state fluorescence spectrum with respect to that of the monomer (Figure 9d), suggests that face-to-face aromatic interactions similar to those encountered in the case of the triester, **3**, are responsible for the excimer emission. However, the presence of a second low-energy, long-living emitting state (~13 ns) suggests that a portion of the aromatic rings in **4** adopt a more planar (sandwich-type) arrangement than in **3**. On the basis of these observations, it seems reasonable to suppose that, in the solid state of the triacid **4**, molecular columns are formed almost exclusively through face-to-face aromatic interactions, whereas the structure is further stabilized by intercolumnar O−H⋯O bonds (see FT-IR spectrum). These interactions presumably "lock" a portion of the aromatic rings of the triacid in a more planar arrangement (sandwich-type).

The analysis of the fluorescence decay traces was made using exponential curve fitting of two exponential terms. The statistical parameter x_v^2 is given in the last column.

Because fluorescence is not sensitive to the extent of stacking, giving essentially the same excimer-like emission spectra for dimers, trimers, etc., we used transmission electron microscopy (TEM) to obtain some estimate of the size of the aggregates formed. Figure 10a shows a typical bright field micrograph of a sample made from an acidic (pH 3) solution of **4**, whereas Figure 10b shows the corresponding micrograph at pH 12. Figure 10a clearly demonstrates elongated ordered domains, indicating molecular organization, with periodicity equal to ca. 0.35 nm, as measured from the diffraction pattern. The organization is lost at high pH values, where only powdery material is observed along with some microcrystallites (Figure 10b). Figure 10c shows a high-resolution bright field micrograph of one of the ribbons of Figure 10a, where the stacking of molecules of **4** is demonstrated with their planes parallel between them and separated from each other by ca. 0.36 nm, as measured directly from the micrograph.

Combined TG/DTA analysis carried out in air on compound **4** (see the Supporting Information) shows a weight loss of 7.5%, corresponding to the departure of two water molecules per formula unit, between ambient temperature and 100 °C. The anhydrous material remains stable up to 320 °C (melting point), indicating that **4** has a robust framework structure, compatible with the findings of spectroscopy and TEM. Finally, X-ray

powder diffraction data showed that the structure was retained upon dehydration (see the Supporting information).

In conclusion, the examination of the crystal packing of various conformationally flexible tri-phenyl-benzene derivatives showed the presence of various types of aromatic interactions in all investigated compounds. However, the formation of columnar structure was observed only when "lateral" hydrogen bonds could be formed to link the columns between them. Moreover, fluorescence (including time-resolved) experiments allowed us to correlate excimer formation in the triester (**3**) and triacid (**4**) compounds with the presence of face-to-face aromatic interactions between parallel rings. Fluorescence measurements in aqueous solutions of the triacid showed that this organization persists even in very dilute solutions, but it collapses in an alkaline environment. This was further verified by TEM experiments. Finally, we assumed that cyclic $O-H\cdots O$ bonds greatly facilitated the formation of low-energy excimers in the triacid (**4**).

Supporting Information Available: Crystallographic data in CIF format and XRPD and TG/DTA data for **4**. This material is available free of charge via the Internet at http://pubs.acs.org.

References

(1) (a) Lehn, J.-M. *Supramolecular Chemistry: Concepts and Perspectives*; VCH: Weinheim, Germany, 1995. (b) Fujita, M., Ed.; *Molecular Self-Assembly*; Structure and Bonding Vol. 96; Springer: Berlin, 2000. (c) Desiraju, G. R., Ed.; *The Crystal as a Supramolecular Entity*; Perspectives in Supramolecular Chemistry Vol. 2; Wiley: Chichester, U.K., 1995. (d) Hollingsworth, M. D. *Science* **2002**, *295*, 2410. (e) Whitesides, G. M.; Grzybowski, B. *Science* **2002**, *295*, 2418. (f) Rogers, R. D., Zaworotko M. J., Eds.; Crystal Engineering. In *Proceedings of the ACA Transactions Symposium*, Arlington, VA, July 18−23, 1998; American Crystallographic Association: Buffalo, NY, 1998; Vol. 33.

(2) (a) Gavezzotti, A. *Acc. Chem. Res*. **1994**, *27*, 309. (b) Gavezzotti, A., Ed.; *Theoretical Aspects and Computer Modeling of the Molecular Solid State*; Wiley & Sons: New York, 1997. (c) Lommerse, J. P. M.; Motherwell, W. D. S.; Ammon, H. L.; Dunits, J. D.; Gavezzotti, A.; Hofmann, D. W. M.; Leusen, F. J. J.; Mooij, W. T. M.; Price, S. L.; Schweizer, B.; Scmidt, M. V.; Van Eijck, B. P.; Verwer, P.; Williams, D. E. *Acta Crystallogr., Sect. B* **2000**, *56*, 697.

(3) Holman, K. T.; Pivovar, A. M.; Ward, M. D. *Science* **2001**, *294*, 1907. (b) Thalladi, V. R.; Brasselet, S.; Blaser, D.; Boese, R.; Zyss, J.; Nangia, A.; Desiraju, G. R. *Chem. Commun.* **1997**, 1841. (c) Frankenbach, G. M.; Etter, M. C. *Chem. Mater.* **1992**, *4*, 272.

(4) Fernandez-Lopez, S.; Kim, H. S.; Choi, E. C.; Delgado, M.; Granja, J. R.; Khasanov, A.; Kraehenbuehl, K.; Long, G. *Nature* **2001**, *412*, 452.

(5) (a) Brunet, P.; Simard, M.; Wust, J. D. *J. Am. Chem. Soc*. **1997**, *119*, 2737. (b) Russel, V. A.; Evans, C. C.; Li, W.; Ward, M. D. *Science* **1997**, *276*, 575. (c) Endo, K.; Sawaki, T.; Koyanagi, M.; Kobayashi, K.; Masuda, H.; Aoyama, Y. *J. Am. Chem. Soc.* **1995**, *117*, 8341.

(6) VanDelden, R. A.; Koumura, N.; Harada, N.; Feringa, B. N. *Proc. Natl. Acad. Sci. U.S.A.* **2002**, *99*, 4945.

(7) Lydon, J. *Curr. Opin. Colloid Interface Sci.* **1998**, *3*, 458.

(8) (a) Etter, M. C. *J. Phys. Chem*. **1991**, *95*, 4601. (b) Ermer, O. *J. Am. Chem. Soc*. **1988**, *110*, 3747. (c) Ermer, O.; Eling, A. *J. Chem. Soc., Perkin Trans*. 2 **1994**, 925.

(9) Sharma, C. V.; Panneerelvam, K.; Pilati, T.; Desiraju, G. R. *J. Chem. Soc., Perkin Trans. 2* **1994**, 2209.

(10) Bernstein, J.; Davey, R. J.; Henck, J.-O. *Angew. Chem., Int. Ed.* **1999**, *38*, 3440.

(11) White, D. J.; Cronin, L.; Parsons, S.; Robertson, N.; Tasker, P. A.; Bisson, A. P. *Chem. Commun*. **1999**, 1107.

(12) The crystal structure of the analogous compound with X = OH has been determined previously by Desiraju et al. (*Chem. Commun.* **2002**, 344). In this case, a closely packed layered structure is obtained by the formation of an unusual seven-membered chain of hydrogen bonds in which OH acts as both hydrogen bond donor and acceptor. This type of packing, in which all available strong and weak donors and acceptors are optimized, follows from the conformational properties of the OH group and the conformational flexibility of the molecule.

(13) Lin, Y. C.; Williams, D. E. *Acta Crystallogr., Sect. B* **1975**, *31*, 318.

(14) Weber, E.; Hecker, M.; Koepp, E.; Orlia, W.; Czugler, M.; Csoregh, I. *J. Chem. Soc., Perkin Trans. 2* **1988**, 1251.

(15) a) Duchamp, D. J.; Marsh, R. E. *Acta Crystallogr., Sect. B* **1969**, *25*, 5. (b) Herbstein, F. H.; Kapon, M.; Shteiman, V. *Acta Crystallogr., Sect. B* **2001**, *57*, 692. (c) Herbstein, F. H.; Marsch, R. E. *Acta Crystallogr., Sect. B* **1977**, *33*, 2358.

(16) The geometrical criterion cited in Lowry T. H.; Richardson., K. S. *Mechanism and Theory in Organic Chemistry*, 3rd ed.; Addison-Wesley: Boston, 1997, for excimer formation via $\pi-\pi$ interactions of aromatic rings is an interplanar angle near 0° and an interplanar distance less than 3.5 Å. Extended aromatic systems interact more strongly than isolated ones. See also: Chen, M.; Ghiggino, K. P.; Smith, T. A.; Thang, S. H.; Wilson, G. J. *Austr. J. Chem*. **2004**, *57*, 1175.

(17) Young, H. K.; Beckerbauer, R. *Macromolecules* **1994**, *27*, 1968.

(18) Beltran, L. M. C.; Cui, C.; Leung, D. H.; Xu, J.; Hollander, F. J. *Acta Crystallogr., Sect. E* **2002**, *58*, 782.

(19) Desiraju, G. R. *Crystal Engineering: The Design of Organic Solids*; Elsevier: Amsterdam, 1989.

(20) Walborsky, H. M.; Barash, L.; Young, A. E.; Impastato, F. J. *J. Am. Chem. Soc*. **1961**, *83*, 2517.

(21) Silverstein, R. S. M.; Bassler, G. C.; Morill, T. C. *Spectrometric Identification of Organic Compounds*, 5th ed.; Wiley & Sons: New York, 1991.

(22) (a) Lu, R.; Jiang, Y. S.; Duo, J. Q.; Chai, X. D.; Yang, W. S.; Lu, N.; Cao, Y. W.; Li, T. J. *Supramol. Sci.* **1998**, *5*, 737. (b) Sielcken, O. E.; Van Tilborg, M. M.; Roks, M. F. M.; Hendriks, R.; Drenth, W.; Nolte, R. J. M. *J. Am. Chem. Soc.* **1987**, *109*, 4261. (c) Kimizuka, N.; Kawasaki, T.; Hirata, K.; Kunitake, T. *J. Am. Chem. Soc.* **1995**, *117*, 7. 6360. (d) Endo, K.; Ezuhara, T.; Koyanagi, M.; Masuda, H.; Aoyama, Y. *J. Am. Chem. Soc.* **1997**, *119*, 9, 499. (e) Marguet, S.; Markovitsi, D.; Millie, P.; Sigal, H.; Kumar, S. *J. Phys. Chem. B* **1998**, *102*, 4697.

(23) (a) Winnik, F. M. *Chem. Rev.* **1993**, *93*, 587. (b) Silva, A. P.; Gunarathe, H. Q. N.; Gunnlaugsson, T.; Huxley, A. J. M.; McCoy, C. P.; Rademacher J. T.; Rice. T. E. *Chem. Rev.* **1997**, *97*, 1515. (c) Yamazaki, I.; Winnik, F. M.; Winnik, M. A.; Tazuke, S. *J. Phys. Chem.* **1987**, *91*, 4213. (d) Tsujii, Y.; Itoh, T.; Fukuda, T.; Miyamoto, T.; Ito S.; Yamamoto, M. *Langmuir* **1992**, *8*, 936. (e) Pistolis, G. *Chem. Phys. Lett.* **1999**, *304*, 371. (f) Itaya, A.; Okamoto, K.; Kusabayashi, S. *Bull. Chem. Soc. Jpn*. **1976**, *49*, 2082.

(24) (a) Mizuno K.; Matsui, A. *J. Lumin.* **1987**, *38*, 323. (b) Sumi. H. *Chem. Phys.* **1989**, *130*, 433.